The Reaction of CH_2OH Radicals with O_2 Studied by Laser Magnetic Resonance Technique

S. Dóbé *, F. Temps, T. Böhland, and H. Gg. Wagner
Max-Planck-Institut für Strömungsforschung, Göttingen

Z. Naturforsch. **40 a**, 1289–1298 (1985); received October 5, 1985

The reaction of CH_2OH with O_2 was studied in an isothermal flow system at 296 K. A rate coefficient, k_1 (296 K) = (6.4 ± 1.5) × 10^{12} cm^3 mol^{-1} s^{-1}, has been determined for the overall reaction

$$CH_2OH + O_2 \rightarrow \text{product(s)} \qquad (1)$$

by monitoring the decay of the LMR signal of the CH_2OH radical. A value of (6.3 ± 2.8) × 10^{12} cm^3 mol^{-1} s^{-1} has been obtained for the overall rate coefficient by following the formation of the product HO_2 radicals in the specific reaction channel

$$CH_2OH + O_2 \rightarrow HO_2 + CH_2O\,. \qquad (1a)$$

No dependence on pressure of k_1 was observed in the pressure range $0.69 \leqq P/\text{mbar} \leqq 6.50$ studied. A complex mechanism has been proposed for the formation of HO_2 and CH_2O in the reaction.

1. Introduction

Hydroxy-methyl radicals (CH_2OH) play an important role in combustion processes and the chemistry of the atmosphere. Under atmospheric conditions the OH-initiated oxidation of ethylene and terminal olefins proceeds through α-hydroxy-alkoxyl radicals which decompose rapidly to CH_2OH radicals [1]. The oxidation of methanol initiated by OH radical attack also leads to CH_2OH [2, 3a, 4, 5]. With the prospect of methanol as an alternative automotive fuel the interest in the mechanism of its oxidation has renewed.

In oxidation systems the fate of CH_2OH is essentially determined by the reaction with O_2. The two most probable reaction routes are hydrogen abstraction (1a) and addition (1b):

$$CH_2OH + O_2 \longrightarrow HO_2 + CH_2O \qquad (1a)$$

$$\xrightarrow[+M]{} OOCH_2OH\,. \qquad (1b)$$

Both the absolute value of the overall rate constant $k_1 = k_{1a} + k_{1b}$ and the branching ratio between the two channels, among other reactions, are of importance in modelling the chemistry of the polluted troposphere. They have a significant effect on the predicted ozone level as well as on the organic product yields [1, 6].

While it is generally accepted that reaction (1) is fast, only very few rate measurements have been performed. The primary obstacle to perform direct studies has been the lack of suitable techniques for the detection of CH_2OH. The recent identification of Laser Magnetic Resonance (LMR) spectra of CH_2OH by Radford et al. [4] has provided a sensitive and selective means for studying its reactions. Recently, mass spectrometry at low electron energies [3, 7, 8] and resonance enhanced multiphoton ionisation spectrometry [9] have also proved to be effective. Another possibility to study reaction (1) is the detection of the product HO_2 [5, 10].

In the present paper we report a direct investigation of reaction (1) using the discharge flow technique combined with LMR. The consumption of CH_2OH and the formation of HO_2 were monitored simultaneously. Overall rate constants were determined from both types of experiments.

2. Experimental

The experimental set up was very similar to that used previously [11]. Here only the special features of the technique are described.

* Permanent address: Central Research Institute for Chemistry, Hungarian Academy of Sciences, H-1025 Budapest, Hungary.

Reprint requests to Prof. Dr. H. Gg. Wagner, Max-Planck-Institut für Strömungsforschung, Bunsenstr. 10, D-3400 Göttingen.

0340-4811 / 85 / 1200-1289 $ 01.30/0. – Please order a reprint rather than making your own copy.

The vertically positioned flow reactor consisted of a 3.9 cm i.d. Pyrex tube of 70 cm length, coated with teflon (Du Pont FEP 856-200). The flow tube was equipped with an inner moveable quartz probe of 15 mm o.d. with radial perforation (1 mm holes) at the end. It contained a second coaxial inner tube (~ 4 mm o.d.) through which CH_3OH was introduced. The distance of the end of the inner tube from the end of the probe was approximately 8 cm.

Hydroxymethyl radicals were generated inside the moveable probe by reacting F atoms with methanol. Fluorine atoms were produced by passing 1% F_2 in He through a microwave discharge burning in an Al_2O_3 insert tube. Methanol in excess was introduced into the coaxial inner tube and was admixed with the F atoms in the lower 8 cm part of the probe. Flow conditions were adjusted to allow for the complete conversion of fluorine atoms into CH_2OH (and CH_3O). The reactant O_2 (or O_2/He mixture) was introduced through a side arm at the upper end of the flow tube.

The decay of CH_2OH and build-up of HO_2 radicals were monitored with a far infrared laser magnetic resonance spectrometer [11]. The following FIR laser lines, lasing gas, CO_2 laser lines, laser polarizations, and magnetic field strengths were applied to detect the radicals:

CH_2OH: $\lambda = 119\,\mu m$, CH_3OH, 9p36, π, $H_0 = 0.04$ Tesla [9], HO_2: $\lambda = 163\,\mu m$, CH_3OH, 10R38, π, $H_0 = 0.23$ Tesla [12].

Among the different CH_2OH transitions reported by Radford et al. [5], the one indicated above proved to be most intense and its symmetric form was of further advantage especially at low signal to noise ratios.

He (Messer Griesheim, 99.999%) served as the main carrier gas. Either pure O_2 (99.998%) or 1.98 (*v*/*v*) % He/O_2 mixture (each Messer Griesheim) were used as reactants. CH_3OH (Merck, 99.7%) was carefully degassed by freeze/thaw cycles prior to use. Special care was taken to remove impurities from the F_2/He line by using a solid NaF and a series of liquid N_2 traps. One of the N_2 (l) traps was attached close to the discharge cavity.

The carrier gas and O_2 flows were measured and regulated with Tylan mass flow controllers. CH_3OH and F_2 flows were regulated by needle valves. Their flow rates could be determined by measuring the pressure rise in calibrated volumes. The total pressure was measured with a pressure transducer (MKS Instruments) downstream of the flow tube.

3. Results

Experiments were carried out at $T = (296 \pm 1)$K in the pressure range of $0.69 \leqq P/\text{mbar} \leqq 6.50$. The average linear flow rates were varied between 9 and 28 m/s. The concentration of F_2 ranged from 1.8×10^{-13} mol/cm^3 to 2.0×10^{-12} mol/cm^3. Methanol concentration was typically about 2×10^{-9} mol/cm^3 calculated for the conditions in the reactor.

The F + CH_3OH reaction used for generating CH_2OH radicals is known to produce also CH_3O radicals in about equal amount [3, 13]. The absolute radical concentrations have not been measured in this study. Computer simulations were made to estimate the initial radical concentrations (see in 3.3). Accordingly, the average initial hydroxymethyl and methoxy radical concentrations were approximately 4.6×10^{-13} mol/cm^3 and 1.3×10^{-12} mol/cm^3, respectively and were varied by about a factor of four.

The O_2 concentration was varied between 3.8×10^{-12} mol/cm^3 and 2.4×10^{-11} mol/cm^3 in the CH_2OH monitoring experiments and was increased up to about 2.5×10^{-10} mol/cm^3 in the HO_2 monitoring runs. At the lowest O_2 concentrations minor corrections had to be made to allow for the oxygen consumption during the reaction.

3.1. Determination of the Overall Rate Coefficient by Monitoring CH_2OH Consumption

The rate constant for the overall reaction

$$CH_2OH + O_2 \rightarrow \text{product(s)} \qquad (1)$$

has been determined by recording the amplitude of the LMR signal of the CH_2OH radical under pseudo first order conditions ($[O_2] \gg [CH_2OH]$) as a function of the reaction time (the position of the moveable probe). Some typical experimental CH_2OH decay curves are shown in Figure 1 a.

In the absence of competitive reactions the decay of $[CH_2OH]$ under pseudo first order conditions is given by the expression

$$-\ln \frac{[CH_2OH]_{+O_2}}{[CH_2OH]_{-O_2}} = -\ln \frac{S(CH_2OH)_{+O_2}}{S(CH_2OH)_{-O_2}} = k_1 [O_2]\, t = k_1^{\psi} t\,, \qquad (A)$$

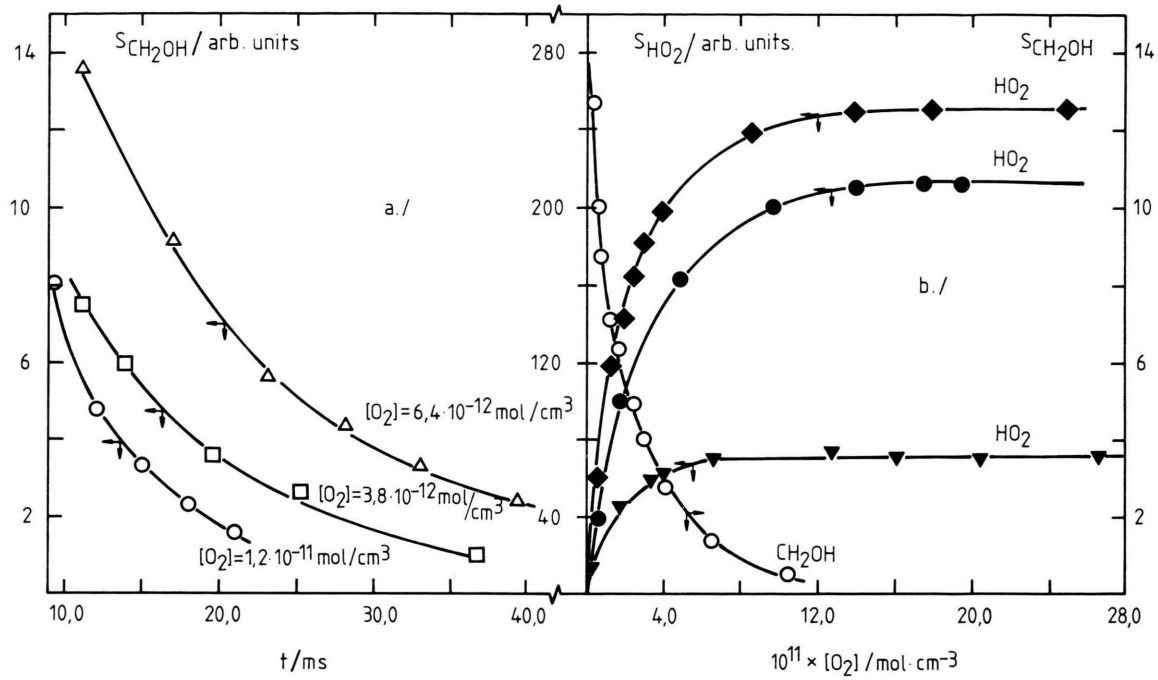

Fig. 1. Typical experimentally measured LMR curves. a) $[CH_2OH]$ decays vs. reaction time, b) $[HO_2]$ build-up as a function of $[O_2]$ at constant ($t = 10.6$ ms) reaction time (for comparison one $[CH_2OH]$ decay curve is also shown). (The approximate $[CH_2OH]_0$ concentrations: ○, ●: 4.3×10^{-13}; □: 3.3×10^{-13}; △, ◆: 6.8×10^{-13}; ▼: 1.8×10^{-13} mol cm^{-3}.)

where $S(CH_2OH)_{+O_2}$ and $S(CH_2OH)_{-O_2}$ are the peak-to-peak amplitudes of the LMR signals of the hydroxymethyl radical in the presence and absence of oxygen, respectively.

In a series of experiments the O_2 concentration was varied between 3.8×10^{-12} mol/cm^3 and 2.4×10^{-11} mol/cm^3 at constant, $P = 2.32 \pm 0.11$ mbar pressure. The experimental conditions are summarized in Table 1. Some typical experimental results are plotted in Fig. 2 according to (A) (solid lines). From the slopes of the straight lines the pseudo first order rate coefficient, k^{ψ}_1 could be obtained. A plot of k_1 vs. O_2 is shown in Figure 3. The full straight line going through the origin represents a least squares fit to the data points, the slope gives a rate coefficient of $k^{\psi}_1 = (6.7 \pm 1.0)\cdot10^{12}$ cm^3 mol^{-1} s^{-1}, with the error limits corresponding to the 95% confidence interval.

The natural logarithm of the amplitudes of the CH_2OH LMR signals plotted vs. the reaction time in the absence of O_2 also gave straight lines. The slopes of the straight lines provided the experimentally measured "effective wall rate coefficients".

Table 1. Experimental conditions for the study of the $CH_2OH + O_2$ reaction ($\bar{T} = 296$ K, $\bar{P} = 2.32$ mbar).

$10^{12}[O_2]_0$ (mol/cm^3)	$10^{13}[F_2]_0$ (mol/cm^3)	$\bar{v}$ (cm/s)	k_w (s^{-1})	k^{ψ}_1 (s^{-1})	$10^{-12}k_1$ (cm^3/mol s)
3.83	12.2	1604	29	23	5.9
6.37	5.3	1734	22	42	6.6
8.45	2.6	1716	22	45	6.7
10.00	1.8	2465	37	62	6.2
12.10	20.0	2071	(64)	73	6.0
15.70	1.8	2756	28	94	6.0
18.10	2.2	2000	30	124	6.9
23.50	12.2	1612	32	161	6.9

Table 2. The overall rate coefficient measured at different pressures.

Pressure (mbar)	0.69	0.93	1.70	2.32[a]	2.95	3.99	6.50
$10^{12}[O_2]_0$ (mol/cm^3)	5.95	4.63	5.48	varied	8.45	7.41	5.52
$10^{-12}k_1$ (cm^3/mol s)	6.1	6.5	7.0	6.7[a]	5.9	5.9	6.7

[a] The average of eight runs.

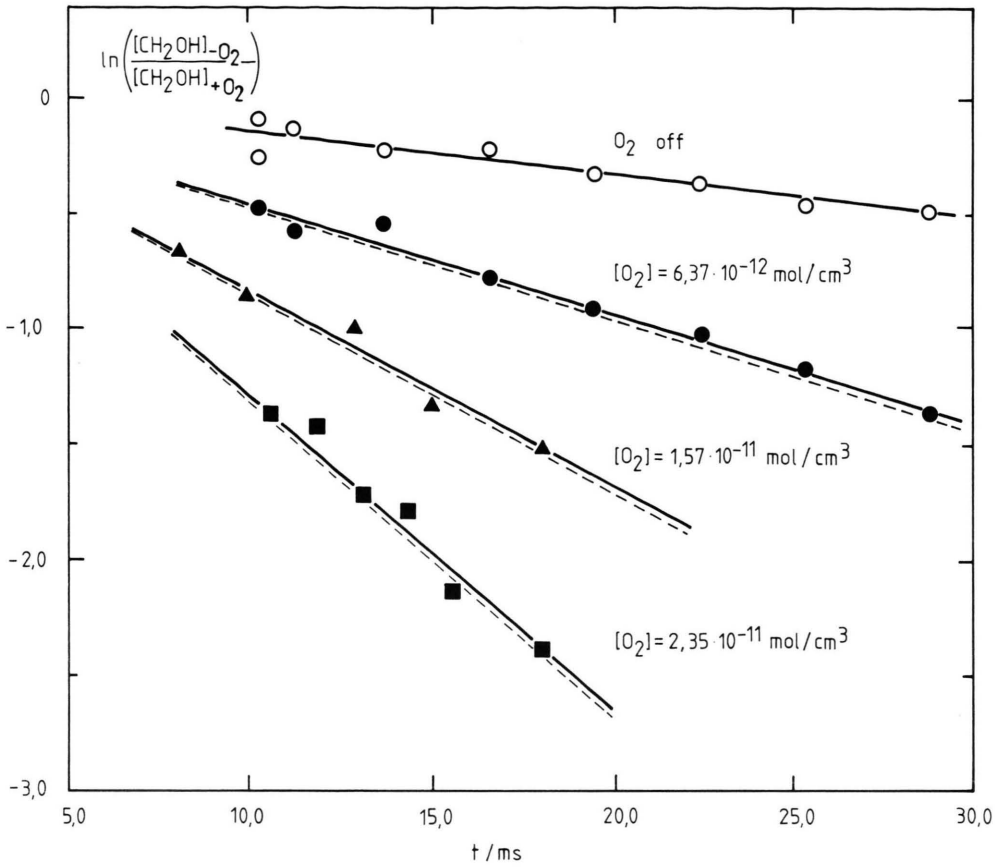

Fig. 2. Some representative pseudo first order $[CH_2OH]$ decays in semilogarithmic plots ($T = 296$ K, $P = 2.31$ mbar). Solid lines: the best fits to the experimental points; dotted lines: the results of computer simulations with $k_1 = 6.4 \times 10^{12}$ $cm^3\ mol^{-1}\ s^{-1}$.

They have been found to be in the range of $k_w^{eff} = 29 \pm 5\ s^{-1}$.

The results of the pressure variation experiments are summarized in Table 2. Only single experiments with one oxygen concentration were carried out at pressures other than 2.32 mbar. The rate coefficients show no systematic variation with pressure in the range studied. It should be mentioned, however, that because of the known difficulties with flow systems [14], only a relatively small pressure range could be covered. Thus, it cannot be precluded that some dependence on pressure of k_1 may exist. A weighted average of the data in Table 2 gave a value of $k_1 = (6.4 \pm 1.0) \times 10^{12}\ cm^3\ mol^{-1}\ s^{-1}$ (the error limits are two standard deviations).

The final results for the overall rate coefficient determined by the decay of the CH_2OH radicals, is: k_1 (296 K) $= (6.4 \pm 1.5) \times 10^{12}\ cm^3\ mol^{-1}\ s^{-1}$ (the error limits are the estimated maximum uncertainties).

3.2. Determination of the Overall Rate Coefficient by Monitoring the Build-up of HO_2

Strong LMR absorption signals of the product hydroperoxyl radicals were observed in the experiments. The formation of HO_2 radicals has been studied with a fixed position of the probe (constant reaction time) by varying the O_2 concentration. The experimental arrangement and data analysis were similar to those used by Radford [5]. Some representative hydroperoxyl LMR signals as a function of $[O_2]$ are given in Figure 1 b. (For comparison one of the CH_2OH decay curves is also shown.) A characteristic feature of all of the HO_2 curves is a limiting HO_2 value reached after the complete

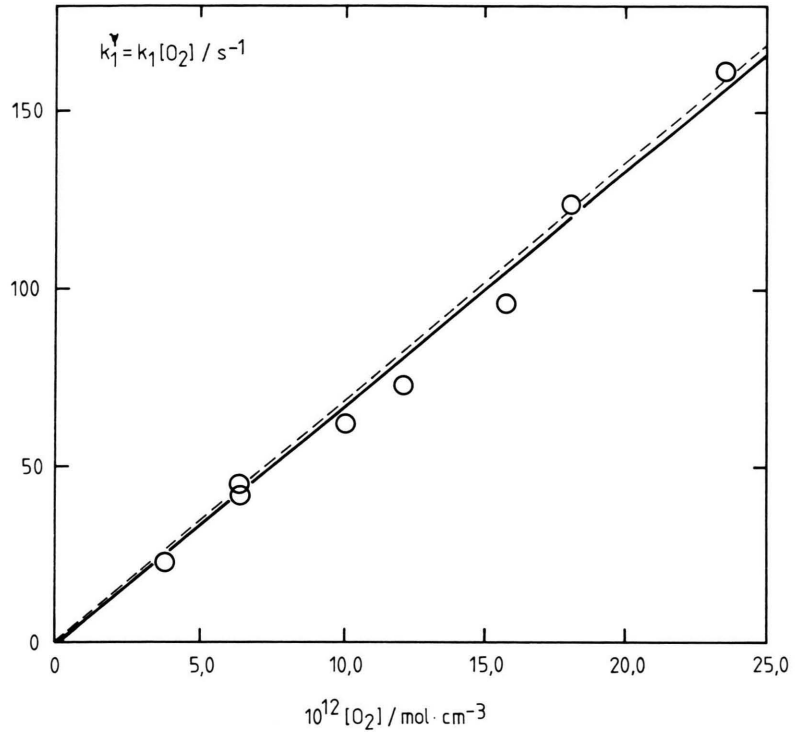

Fig. 3. Pseudo first order rate coefficient, k_1^{ψ} as a function of the O_2 concentration ($T = 296$ K, $P = 2.31$ mbar). Solid line: the best fit to the experimental points; dotted line: the result of computer simulations with $k_1 = 6.4 \times 10^{12}$ cm^3 mol^{-1} s^{-1}.

conversion of the CH_2OH radicals. The amplitudes of these maximal signals remained constant while moving the probe towards larger distances. This behaviour has been observed also by Radford and means that the HO_2 radical is a "stable product" with the time-scale employed. (The different $S_{HO_2}^{max}$ boundary values in Fig. 1 b reflect the differences in the initial CH_2OH concentrations.)

No HO_2 signals could be detected in the absence of O_2 indicating the vacuum-tightness of the system. The measurability of the HO_2 radicals was significantly better than that of the CH_2OH radicals because of the greater sensitivity of the LMR spectrometer towards HO_2.

A rate coefficient can be derived for the overall reaction from the measured HO_2 signals, evaluating the relative intensities ($S_{HO_2}/S_{HO_2}^{max}$) at different oxygen concentrations. The following expression is obtained from mass-balance considerations, after the integration of the rate equations (see also in [5]):

$$\frac{S_{HO_2}}{S_{HO_2}^{max}} = \frac{1 - \exp\{-(k_1[O_2] + k_w)\, t\}}{1 + \dfrac{k_w}{k_1[O_2]}}. \qquad \text{(B)}$$

A least squares fitting computer program was used to estimate k_1. All of the $S_{HO_2}/S_{HO_2}^{max} - [O_2]$ data pairs from different experiments were taken in one fitting procedure with the average $k_w = 29$ s^{-1} and $t = 10.6$ ms parameters. (Because of the increased uncertainties, the data points with $S_{HO_2}/S_{HO_2}^{max} > 0.80$ have been omitted.) The fitted (solid)curve together with the experimental points are shown in Figure 4. The rate coefficient obtained with the combined statistical and estimated systematic errors is

$$k_1 = (6.3 \pm 2.8) \times 10^{12} \text{ cm}^3 \text{ mol}^{-1} \text{ s}^{-1}.$$

In (B) the absolute value of the reaction time is needed, which is a badly definable quantity in LMR-flow tube combinations. Mainly this is reflected in the relatively large error limits of the rate coefficient given.

Corrections in the rate coefficients for viscous pressure drop and axial diffusion have been taken into account by known formulas [14] in both types of measurements. Their maximum contributions were less than 2 and 11%, respectively.

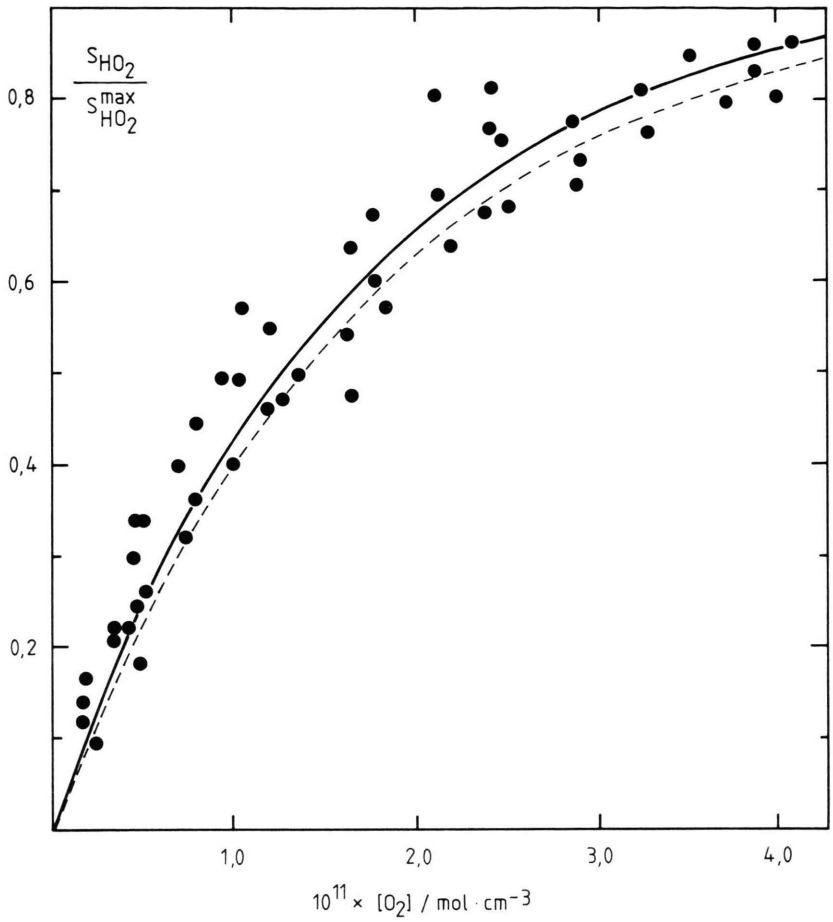

Fig. 4. Estimation of k_1 according to (B) (solid curve); the result of computer simulations with $k_1 = 6.4 \times 10^{12}\,cm^3\,mol^{-1}\,s^{-1}$ (dotted curve).

3.3. The Significance of Side Reactions

The linearity of the plots in Figs. 2 and 3 and the zero intercept in Fig. 3 indicate that consecutive and parallel reactions cannot be significant under our experimental conditions. Among the side reactions the radical-radical reactions are thought to play some role. The experimentally measured "effective wall rate constant" presented a slight increase with increasing initial radical concentration, from which a $20\,s^{-1}$ "true wall rate constant" and a rate coefficient of about $1 \times 10^{13}\,cm^3\,mol^{-1}\,s^{-1}$ for the self-combination reaction of the CH_2OH radicals could be estimated. The latter is in good agreement with the value reported by Grotheer et al. [8]. So, the decay of CH_2OH without O_2 in greater part can be due to heterogeneous processes, in which case the on-off technique directly corrects for the side reactions [15].

In order to further asses the importance of the possible interfering reactions we have carried out computer simulations with the reactions and rate coefficients summarized in Table 3 by using the computer routine of [16]. As a first step, the initial radical concentrations were calculated by modelling the reactions inside of the movable probe (steps (2)–(10)). The dissociation of F_2 in the microwave discharge was taken to be complete and the wall recombination of F atoms was neglected [17]. The other possible reactions of HO_2 in the reactor have been omitted on the basis of the experimental findings that the HO_2 radical behaved as a "stable product" in the system after the complete conversion of CH_2OH into HO_2.

The modelling of the $[CH_2OH]$ decays yielded practically identical results with the results of the usual pseudo first order analysis of the experimentally measured CH_2OH LMR signals when the

Table 3. Reactions used in the model calculations.

Reaction		k (296 K) cm^3, mol, s units	Ref.
$CH_2OH + O_2 \rightarrow HO_2 + CH_2O$	(1)	k_1 = varied	
$F + CH_3OH \rightarrow CH_2OH + HF$	(2a)	$k_{2a} + k_{2b} = 5 \times 10^{13}$	estim.
$\rightarrow CH_3O + HF$	(2b)	$k_{2a}/k_{2b} = 0.7$	[2]
$F + CH_2OH \rightarrow HF + CH_2O$	(3)	$k_3 = 1 \times 10^{14}$	estim.
$F + CH_3O \rightarrow HF + CH_2O$	(4)	$k_4 = 1 \times 10^{14}$	estim.
$2\,CH_2OH \rightarrow$ prod.	(5)	$k_5 = 9.0 \times 10^{12}$	[8]
$CH_3O + CH_2OH \rightarrow CH_3OH + CH_2O$	(6)	$k_6 = k_5$	assumed
$CH_2OH + CH_3OH \rightarrow CH_3O + CH_3OH$	(7)	$k_7 = 7 \times 10^4$	estim. [a]
$CH_3O + CH_3OH \rightarrow CH_2OH + CH_3OH$	(8)	$k_8 = 2 \times 10^6$	estim. [b]
$CH_2OH \rightarrow$ wall prod.	(9)	$k_9 = k_w = 20$	this work
$CH_3O \rightarrow$ wall prod.	(10)	$k_{10} = k_9$	assumed
$CH_2OH + HO_2 \rightarrow$ prod.	(11)	$k_{11} = 3.6 \times 10^{13}$	[8]
$CH_3O + HO_2 \rightarrow CH_3OH + O_2$	(12)	$k_{12} = 1.0 \times 10^{12}$	[8]
$CH_3O + O_2 \rightarrow HO_2 + CH_2O$	(13)	$k_{13} = 1.1 \times 10^9$	[3b]
$HO_2 + CH_2O \rightarrow$ prod.	(14)	$k_{14} = 1 \times 10^{10}$	[25]

[a] The rate coefficient of the reaction: $CH_3 + CH_3OH \rightarrow CH_4 + CH_3O$ [29].
[b] The rate coefficient of the reaction: $CH_3O + C_2H_6 \rightarrow CH_3OH + C_2H_5$ [29].

$k_1 = 6.4 \times 10^{12}$ cm^3 mol^{-1} s^{-1} rate coefficient was used as an input parameter in the simulations (compare the solid and dotted lines in Figs. 2 and 3). Similarly, the best agreement was found between the the experimentally measured and calculated $[HO_2]/[HO_2]^{max}$ ratios when k_1 was chosen to be in the range of $(6.0-6.7) \times 10^{12}$ cm^3 mol^{-1} s^{-1} (in Fig. 4 the dotted curve shows the result of a simulation carried out with $k_1 = 6.4 \times 10^{12}$ cm^3 mol^{-1} s^{-1}).

The later model calculations have also justified the use of (B) in deriving k_1 at our low radical concentrations (cf. the dotted and solid curves in Figure 4).

4. Discussion

The rate coefficients determined by monitoring the decay of CH_2OH radicals and the formation of HO_2 radicals with the LMR technique in a flow system at 296 K are

$$k_1 = (6.4 \pm 1.5) \times 10^{12}\ \text{cm}^3\ \text{mol}^{-1}\ \text{s}^{-1}$$

and

$$k_1 = (6.3 \pm 2.8) \times 10^{12}\ \text{cm}^3\ \text{mol}^{-1}\ \text{s}^{-1},$$

respectively. They are in excellent agreement with each other.

There are only a few direct studies of reaction (1) known from the literature. Two investigations have been carried out by directly monitoring the hydroxymethyl radicals. Shortly after the description of the LMR spectra of CH_2OH by Radford et al. [4], Rohrbeck, Radford, and Fortuño [18] reported a value of $k_1 = (1.5 \pm 0.2) \times 10^{12}$ cm^3 mol^{-1} s^{-1} at room temperature. In a very recent study at 300 K in a flow system using mass spectrometric detection of CH_2OH radicals, Grotheer et al. [8] obtained $k_1 = (5.7 \pm 1.5) \times 10^{12}$ cm^3 mol^{-1} s^{-1}. While the very recent mass spectrometric results are in excellent agreement with our k_1 value, the value of Rohrbeck et al. disagrees.

In the study of Rohrbeck et al. the experimental arrangement probably was very similar to ours (flow tube technique, LMR detection of the CH_2OH radicals, pseudo first order conditions, etc.). In their study a "clean" CH_2OH source, the reaction of Cl atoms with methanol [19] was used. Searching for the cause of discrepancy, we have carried out a few experiments using the $Cl + CH_3OH$ reaction to generate CH_2OH radicals. The average of rate coefficient derived was 5.9×10^{12} cm^3 mol^{-1} s^{-1}, in good agreement with our value obtained with the $F + CH_3OH$ radical source. Thus, at the present stage we can not offer any reasonable explanation for the discrepancy.

In another group of investigations reaction (1) was studied by detecting the reaction product HO_2. A common feature of these investigations is the use of (B) in evaluating k_1. The earliest work was made by Radford [5] at room temperature with the LMR-flow tube combination technique. The measurement

of the relative intensities of the LMR signals as a function of $[O_2]$ allowed a rate coefficient of $(1.2^{+1.2}_{-0.6}) \times 10^{12}$ cm^3 mol^{-1} s^{-1} to be derived. Recently Wang et al. [10] have studied the $CH_2OH + O_2$ reaction in a flow system at room temperature by detecting the HO_2 radicals from photofragment emission. In this way a rate coefficient of $(8.4 \pm 2.4) \times 10^{11}$ cm^3 mol^{-1} s^{-1} has been determined. The above two values are five to eight times lower than the rate coefficient obtained by the very similar treatment of the experimental data in the present work. It is to be noted, however, that the derivation of (B) is based on the assumption that the only important reactions are reaction (1) and the wall consumption of CH_2OH. Evidently, this can be the case only at low radical concentrations. At higher radical concentrations the use of (B) can lead to underestimation of k_1 as was shown by Grotheer et al. [8] discussing Radford's low rate coefficient. Similar arguments can be advanced in connection with the study of Wang and coworkers. The CH_2OH concentrations in their system seem to have been at least one order of magnitude higher than those in the present work. Under such conditions the radical-radical reactions of CH_2OH and HO_2 may have played a not negligible role.

In the present study practically the same rate coefficient was found by monitoring either the consumption of CH_2OH or the build up of HO_2 radicals. In the second case the product of a single reaction channel is monitored, and this may give the impression that the rate coefficient of a specific reaction route is measured. It is to be noted, however, that information can be gained only on the overall rate coefficient with the methods applied here.

The formation of $HO_2 + CH_2O$ appears to be the only reaction channel from product analysis and Fourier-transform spectroscopic studies. No indications were found for the occurrence of the combination reaction of CH_2OH with O_2 during the OH initiated oxidation of ethylene and in the study of photochemical oxidation of alcohols under simulated atmospheric conditions [1, 20]. On the other hand, there has been conclusive evidence from the studies of the reverse reaction, the addition of HO_2 to CH_2O, for the existence and relative stability of the $OOCH_2OH$ radical which is the expected combination product in the $CH_2OH + O_2$ reaction. In the study of the photochemical oxidation of formaldehyde, Su et al. [21] and Niki et al. [22] identified the compound hydroxymethyl-hydroperoxide ($HOOCH_2OH$) by the FTIR spectroscopy and explained its formation through the hydroxymethyl-peroxy radical. From these studies a general picture has emerged for the photochemical oxidation of CH_2O in the atmosphere. The first steps are the addition and the fast rearrangement of the adduct formed into the more stable $OOCH_2OH$ radical:

$$HO_2 + CH_2O \rightarrow HOOCH_2O \qquad (-D)$$

$$HOOCH_2O(+M) \rightarrow OOCH_2OH(+M)$$

We suggest a consistent though basically qualitative interpretation for the reaction of CH_2OH with O_2 which is in accordance with the results of the formaldehyde oxidation studies. The reaction is assumed to proceed via a "complex" mechanism:

$$CH_2OH + O_2 \underset{(-C)}{\overset{(C)}{\leftrightarrows}} (OOCH_2OH)^* \underset{(-I)}{\overset{(I)}{\leftrightarrows}} (OCH_2OOH)$$

$$(OOCH_2OH)^* \xrightarrow{[M]} OOCH_2OH \quad (S)$$

$$(OOCH_2OH)^* \xrightarrow{(D)} HO_2 + CH_2O \quad (-D)$$

$$(OCH_2OOH) \xrightarrow{(D)} HO_2 + CH_2O \quad (-D)$$

In the first step the vibrationally excited $(OOCH_2OH)^*$ radical is formed with about 137 kJ/mol excess energy. (The complex formation has been found to be the dominant pathway in the reaction of O_2 with C_2H_5, which is isoelectronic with the hydroxymethyl radical [23].) In principle, the "chemically activated" $(OOCH_2OH)^*$ adduct can decay by three different routes: redissociation (−C), stabilization (S) and isomerization through 1,4 hydrogen atom transfer (I). The energetics of the reactions have been schematically illustrated in Figure 5.

The stabilization route may not play a significant role because no pressure dependence was observed in our experiments. An activation energy for the $OOCH_2OH \xrightarrow{(I)} OCH_2OOH$ rearrangement can be estimated by the rate coefficient $k_{(I)} = 1.5$ s^{-1} determined by Su et al. [20] during the study of formaldehyde oxidation. Accepting $A_{(I)}$ to be equal to $10^{11.2}$ s^{-1}, the preexponential factor for a five membered transition-state reaction [24], $E_{(I)} = 63$ kJ/mol activation energy can be calculated. The significant difference in the barrier heights makes the isomerization of the $OOCH_2OH$ radical favourable to the redissociation. The last step in the scheme,

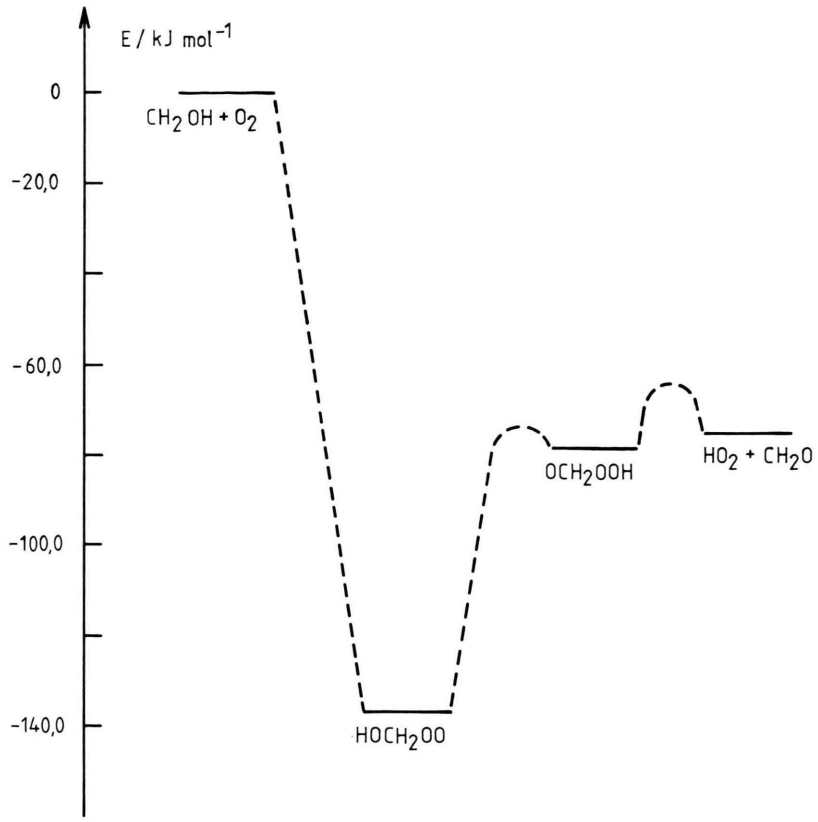

Fig. 5. Energy diagram for $CH_2O + HO_2$ formation in the reaction of CH_2OH with O_2. (The standard reaction enthalpies have been calculated mainly by group additivity rules [26], $\Delta H^{\ominus}_{f,298}$ values of CH_2OH and HO_2 were taken from [27] and [28], respectively.)

the decomposition of the isomerized $HOOCH_2O$ radical, is practically thermoneutral. Its activation energy must be small according to the high rate coefficients measured for the reverse reaction (see e.g. $k_{(-D)} = 6.9 \times 10^9$ cm^3 mol^{-1} s^{-1} [21] or $k_{(-D)} = 1.0 \times 10^{10}$ cm^3 mol^{-1} s^{-1} [25]). The $HOOCH_2O$ radical still may have some excess energy and decompose in a fast step to HO_2 and CH_2O.

It follows from the kinetic considerations made above that the measured rate coefficient is equal to the rate coefficient of the combination reaction, i.e.: $k_1 = k_{(C)}$ and the reaction proceeds through fast consecutive steps which are the reverse steps of the HO_2 addition to formaldehyde. The intermediate $OOCH_2OH$ radical has significantly more excess energy when formed in the $CH_2OH + O_2$ reaction than when it is formed in the $HO_2 + CH_2O$ reaction. This difference in energy can explain why the characteristic $HOOCH_2OH$ product could be observed in the $HO_2 + CH_2O$ investigations whereas no indication was found for it in the $CH_2OH + O_2$ studies.

Acknowledgement

We thank the Fonds der Chemie for financial support of these investigations. S. Dóbé gratefully acknowledges a stipendium granted by the Max-Planck-Gesellschaft for 1983–84. The authors wish to thank Mr. T. Turányi for making the computations.

[1] H. Niki, P. D. Maker, C. M. Savage, and L. D. Breitenbach, J. Phys. Chem. **82,** 135 (1978).
[2] U. Meier, H. H. Grotheer, and Th. Just, Chem. Phys. Lett. **106** (1) (1984).
[3] a) J. Hägele, K. Lorenz, D. Rhäsa, and R. Zellner, Ber. Bunsenges. Phys. Chem. **87,** 1023 (1983). b) K. Lorenz, D. Rhäsa, R. Zellner, and B. Fritz, Ber. Bunsenges. Phys. Chem. **89,** 341 (1985).
[4] H. E. Radford, K. M. Evenson, and D. A. Jennings, Chem. Phys. Lett. **78** (3), 589 (1981).
[5] H. E. Radford, Chem. Phys. Lett. **71(2),** 195 (1980).
[6] R. Atkinson and A. C. Lloyd, J. Chem. Phys. Ref. Data **13(2),** 315 (1984).
[7] K. Hoyerman, N. S. Loftfield, R. Sievert, and H. Gg. Wagner, 18th Symp. (Int.) Combustion, Proc. **1981,** 831.
[8] H. H. Grotheer, G. Riekert, U. Meyer, and Th. Just, Ber. Bunsenges. Phys. Chem. **89,** 187 (1985).
[9] C. S. Dulcey and J. W. Hudgens, J. Phys. Chem. **87,** 2296 (1983).
[10] W. C. Wang, M. Suto, and L. C. Lee, J. Chem. Phys. **81,** 3122 (1984).
[11] a) F. Temps, Ph.D. thesis, MPI f. Strömungsforschung Report 4/1983, Göttingen 1983. b) F. Temps and H. Gg. Wagner, Ber. Bunsenges. Phys. Chem. **88,** 410 (1984).
[12] R. M. Stimpfle, R. A. Perry, and C. J. Howard, J. Chem. Phys. **71,** 5183 (1979).
[13] K. H. Hoyermann and T. Khatoon, to be published.
[14] F. Kaufman, Prog. React. Kinet. **1,** 3 (1961).
[15] K. H. Hoyerman, in "Physical Chemistry-An Advanced Treatise. Vol. VI.B/Kinetics of Gas Reactions", Chapter 12, Academic Press, New York 1975.
[16] B. A. Gottwald and G. Wanner, Computing **26,** 355 (1981).
[17] C. D. Walther and H. Gg. Wagner, Ber. Bunsenges. Phys. Chem. **87,** 403 (1983).
[18] W. Rohrbeck, H. E. Radford, and G. Fortuño, 15th Int. Symp. on Free Radicals, Ingonish Beach, Canada 1981.
[19] J. W. Michael, D. F. Nava, W. A. Payne, and L. J. Stief, J. Chem. Phys. **70(8),** 3652 (1970).
[20] W. P. L. Carter, K. R. Darnall, R. A. Graham, A. M. Winer, and J. N. Pitts, Jr., J. Phys. Chem. **83,** 2305 (1979).
[21] Fu Su, J. G. Calvert, and J. H. Shaw, J. Phys. Chem. **83,** 3185 (1979).
[22] H. Niki, P. D. Maker, C. M. Savage, and L. P. Breitenbach, Chem. Phys. Lett. **75,** 533 (1980).
[23] J. C. Plumb and K. R. Ryan, Int. J. Chem. Kinet. **13,** 1011 (1981).
[24] A. C. Baldwin, J. R. Barker, D. M. Golden, and D. G. Hendry, J. Phys. Chem. **81,** 2483 (1976).
[25] F. Temps, unpublished result.
[26] S. W. Benson, Thermochemical Kinetics, 2nd. Ed., John Wiley, New York 1976.
[27] D. M. Golden and S. W. Benson, Chem. Rev. **69,** 125 (1969).
[28] L. G. S. Shum and S. W. Benson, J. Phys. Chem. **87,** 3479 (1983).
[29] J. A. Kerr and S. J. Moss, CRC Handbook of Bimolecular and Termolecular Gas Reactions, CRC Press, Inc., Boca Raton, Florida 1981.